



1 Refined classification and characterization of atmospheric new particle 2 formation events using air ions

3 Lubna Dada^{1*}, Robert Chellapermal¹, Stephany Buenrostro Mazon¹, Pauli Paasonen¹, Janne Lampilahti¹,
4 Hanna E. Manninen^{1,2}, Heikki Junninen^{1,3}, Tuukka Petäjä^{1,4}, Veli-Matti Kerminen¹, and Markku
5 Kulmala^{1,4,5}

6 ¹Institute for Atmospheric and Earth System Research, University of Helsinki, Helsinki, Finland

7 ²Experimental Physics Department, CERN, 1211 Geneva, Switzerland

8 ³Institute of Physics, University of Tartu, Ülikooli 18, EE-50090 Tartu, Estonia

9 ⁴Aerosol and Haze Laboratory, Beijing Advanced Innovation Center for Soft Matter Science and Engineering, Beijing
10 University of Chemical Technology, Beijing, China

11 ⁵Joint International Research Laboratory of Atmospheric and Earth System Sciences, Nanjing University, Nanjing, China

12 *Correspondence to: Lubna Dada (lubna.dada@helsinki.fi)

13 **Abstract.** Atmospheric new particle formation (NPF) is a world-wide observed phenomenon that affects the human health
14 and the global climate. With the growing network of global atmospheric measurement stations, efforts towards investigating
15 NPF have increased. In this study, we present an automated method to classify days into four categories including NPF events,
16 non-events and two classes in between, which then ensures the reproducibility and minimizes the man-hours spent on manual
17 classification. We applied our automated method to 10 years of data collected at the SMEAR II measurement station in
18 Hyytiälä, southern Finland. In contrast to the traditionally-applied classification methods which categorize days into events,
19 non-events and ambiguous days as undefined days, our method is able to classify the undefined days as it accesses the initial
20 steps of NPF at sub-3 nm sizes. Our results show that on ~24% of the days in Hyytiälä, a regional NPF event occurred and
21 was characterized by a ‘nice weather’ and favorable conditions such as a clear sky and low condensation sink. Another class
22 found in Hyytiälä is the transported event class, which seems to be NPF carried horizontally or vertically to our measurement
23 location and it occurred on 17% of the total studied days. Additionally, we found that an ion burst, where the ions apparently
24 fail to grow to larger sizes, occurred on 18% of the days in Hyytiälä. The transported events and ion bursts were characterized
25 by less favorable ambient conditions than regional NPF events, and thus experienced interrupted particle formation or growth.
26 Non-events occurred on 41 % of the days and were characterized by a complete cloud cover and high relative humidity.
27 Moreover, for the regional NPF events occurring at the measurement site, the method identifies the start time, peak time and
28 end time, which helps us focus on variables within an exact time window to better understand NPF in a process level. Our
29 automated method can be modified to work in other measurement locations where NPF is observed.

30 Keywords: NPF events, air ions, intermediate ions, boreal forest

31



32

33 **1 Introduction**

34 New particle formation (NPF) is an atmospheric phenomenon that results in a big addition to aerosol load in the global
35 troposphere Spracklen et al. (2010); Kerminen V-M. (2018). NPF is observed frequently in different environments around the
36 globe, ranging from pristine locations (Siberia –Kulmala et al. (2011); Asmi et al. (2016)), to boreal forests (Hyytiälä -Kulmala
37 et al. (2013); Nieminen et al. (2014)), tropical forests (Amazon -Artaxo et al. (2013); Wimmer et al. (2017)), mountain tops
38 (Jungfraujoch–Bianchi et al. (2016)), semi-polluted cities (European cities -Manninen et al. (2010)) and even heavily polluted
39 mega cities (China -Kulmala et al. (2016); (2017); Wang et al. (2017)). The freshly formed particles that grow to larger sizes
40 contribute largely to the cloud condensation nuclei load in the atmosphere (Merikanto et al., 2009; Kerminen et al.,
41 2012; Salma et al., 2016) and thus indirectly affect the climate.

42 In order to comprehend the phenomenon of NPF in a specific location, we first need to understand its frequency and
43 characteristics as well as particle formation and growth rates associated with it. With the growing number of global stations
44 (Kulmala, 2018), an automatic method is needed to classify the days into events and non-events. In addition to minimizing
45 the effort of manual event classification, an automated method tends also to reduce any human error. In this study, we present
46 an automated method which classifies days into four classes according to the observed characteristics of 2–4 nm sized air ions
47 and 7–25 nm sized particles. The original classification method of days as events, non-events and undefined days was proposed
48 by (Dal Maso et al., 2005), and later modified by (Kulmala et al., 2012), and is based on particle measurements starting from
49 about 3 nm in particle mobility diameter, thus missing the initial steps of NPF. With the increased development of
50 instrumentation, we are able to access sub-3 nm clusters and refine our classification method to account for the very initial
51 steps of NPF. The classification proposed here divides days into regional events, transported events, ion bursts and non-events,
52 thus excluding any ‘undefined’ days, which minimizes the number of days usually excluded from further data analysis.
53 Furthermore, our automated method identifies the start, peak and end time of daytime regional events or ion bursts. By
54 identifying the start and end times, we are able to concentrate on the conditions present during the actual NPF time window.

55 Our study focuses on the NPF occurring in Hyytiälä, a boreal forest site in southern Finland where the SMEAR II (Station for
56 Measuring Forest Ecosystem-Atmosphere Relations) measurement station is located (Hari and Kulmala, 2005). The dataset
57 collected at the station sums up more than 22 years of particle, meteorological and gas data, making extensive analyses of
58 NPF and related parameters possible. Besides studying NPF occurrence in Hyytiälä, our method can be applied to other
59 locations where NPF is observed, enabling scientists studying particle formation to focus on specific time windows by which
60 active NPF occurs. Our specific aims in this study are i) to automatically classify days in Hyytiälä according to their initial
61 NPF steps, ii) to minimize the number of undefined days by refining the classification, iii) to investigate different
62 characteristics of classified days, iv) to identify the start, peak and end times of regional events and, thereby, v) to create a
63 time series which allows us to focus on the exact time period during which a regional new particle formation event has
64 occurred.

65



66 2 Materials and Methods

67 2.1 Measurement location

68 The main results of our study are based on the measurements collected at the SMEAR II) station located in the boreal forest
69 site in Hyytiälä, Southern Finland (61°51'N, 24°17'E, 181 m a.s.l). The station has accumulated 22 years of comprehensive
70 measurements including particle, radiation, gas, meteorological and complementary data. The location is considered a semi-
71 clean boreal forest environment as it is far from anthropogenic pollutants (Asmi et al., 2011) and thus represents the northern-
72 hemisphere boreal forests. A more detailed description of the site and the ongoing measurements can be found in Hari and
73 Kulmala (2005) and Nieminen et al. (2014).

74 2.2 Instrumentation

75 The traditional classification of days as NPF events and non-events follows the method proposed by Dal Maso et al. (2005);
76 Kulmala et al. (2012). For this classification method, the particle number-size distributions measured with a twin-DMPS
77 (Differential Mobility Particle Sizer) system (Aalto et al., 2001), were used. The twin DMPS system measured the aerosol
78 number-size distribution over the size range 3-500 nm until 2004 and over the size range 3-1000 nm from 2005 onwards. The
79 DMPS measurements are also used to calculate the condensation sink (CS) which is the rate at which non-volatile vapors
80 condense onto a pre-existing particles (Kulmala et al., 2012).

81 For our proposed automated classification method, the mobility distributions of charged and neutral aerosol particles and
82 clusters in the size range of 0.8–47 nm and 2–42 nm, respectively, were measured with a Neutral cluster and Air Ion
83 Spectrometer (NAIS, Airel Ltd., Estonia, (Manninen et al., 2016; Manninen et al., 2009; Mirme and Mirme, 2013) between
84 2006 and 2015. No measurements using the NAIS were made during year 2008 when the instrument was used for an intensive
85 campaign. Particle and air ion data are available in two-minute time steps.

86 The air temperature and the relative humidity are measured with 4-wired PT-100 sensors and relative humidity sensors
87 (Rotronic Hygromet MP102H with Hygroclip HC2-S3, Rotronic AG, Bassersdorf, Switzerland) on a mast at a height level of
88 16.8 m, respectively. The temperature and relative humidity data are provided as 30-minute averages. Solar radiation in the
89 wavelengths of global radiation (0.30-4.8 μm) is monitored using pyranometers (SL 501A UVB, Solar Light, Philadelphia,
90 PA, USA; Reeman TP 3, Astrodata, Tõravere, Tartumaa, Estonia until June 2008, and Middleton Solar SK08, Middleton
91 Solar, Yarraville, Australia since June 2008) above the forest at 18 m. We used global radiation data for calculating the
92 cloudiness parameter (P), which is the ratio of global radiation to theoretical maximum radiation arriving at Hyytiälä, by
93 following the method proposed by Dada et al. (2017). Values of $P \leq 0.3$ represent a complete cloud cover while values of P
94 ≥ 0.8 can be considered to represent clear-sky conditions.

95 2.3 Event classification decision tree

96 Based on the concentrations of 2 – 4 nm ions, we are able to detect the initial steps of cluster formation (see Leino et al.
97 (2016)), which would not be possible using the DMPS system alone and the traditional classification. This small size window
98 available from the NAIS operating in ion mode gives an additional opportunity to investigate sub-3 nm clusters. Accordingly,
99 we are able to estimate whether a regional NPF event occurred within the air mass in which the observations were made, or
100 elsewhere and then carried to our measurement location. Similarly, undefined days are identified based on their sub-3 nm
101 characteristics. We present in Figure 1 our refined classification decision tree and apply it to Hyytiälä data in this study. In
102 order to attain this classification, we rely on the initial steps of cluster formation and their further growth, which we monitor
103 using an automatic method. Since in our study we are interested in daytime NPF, we chose the time window between 06:00
104 and 19:00 when monitoring aerosol number concentrations. However, the automated method can be tweaked to include
105 evening or night time event classification in places where these event types are present.

106 Our decision tree (Figure 1) first examines 2–4 nm ion concentrations representing the initial step of new particle formation.
107 A notable increase in their concentration is interpreted as ion clustering on site. To be accounted as an increase, the number
108 concentration of ions after 06:00 must increase above a relative threshold and persist for more than 1 hour. This threshold is
109 calculated from ion concentration averaged over the time period 00:00–04:00 multiplied by a scaling factor (Figure 2A); we
110 chose this time window as background as it is outside the time window when night time ion clusters are observed (Buenrostro
111 Mazon et al., 2016; Rose et al., 2018). To be accounted as a notable increase past the threshold value, a concentration of 20



112 ions/cm³ should be reached and should last for at least 1 hour. We chose the aforementioned value as it has been found to be
113 an indicator for NPF in Hyttiälä (Leino et al., 2016). If this criterion is met, these ions are expected to either grow into bigger
114 sizes and lead to regional NPF events (RE), or fail to grow further, in which case the event are identified as ion bursts (IB)
115 that do not form new particles.

116 To decide whether the particle growth is observed, particle concentrations in the size range of 7 – 25 nm are examined. These
117 particles represent the growth phase of freshly-formed clusters. Since in Hyttiälä growth rates of 4 – 7 nm particles is reported
118 to lie between 0.8 and 17 nm/h (Average 3.8 nm/h) (Yli-Juuti et al., 2011), we considered a time delay of 1 to 8 hours between
119 the initial increase of ion (2 – 4 nm) concentrations and particle (7 – 25 nm) concentrations. To be considered as an increase,
120 the particle number concentration should exceed a relative threshold which in this case is the number concentration averaged
121 over the time period of 03:00–05:00 (Figure 2B). We determined the background time window by comparing the automatic
122 method to a manual classification that we performed for the years 2013–2014 from our data set. The increase in concentration
123 should last for ~1.5 hr (100 minutes) and reach a peak of at least 3000 particles/cm³. On one hand, if both 2 - 4 nm ions and
124 7 – 25 nm particles are present, the time period is considered as a regional event (RE). On the other hand, if the 2 - 4 nm ions
125 are present but they do not grow to form 7 – 25 nm particles, the time period is classified as an ion burst (IB). Moreover, if 2
126 – 4 nm ions are not present, but we observe an increase in the particles, this leads to the assumption that the NPF event did
127 not occur at the measurement location but was carried horizontally or vertically to our site (Leino et al., 2018). The latter has
128 been previously described as a tail event (Buenrostro Mazon et al., 2009) or a transported event (TE). However, if neither
129 criterion is met, which means that neither 2 – 4 nm ions nor 7 – 25 nm particles are present in sufficient concentrations, the
130 time period is then classified as a non-event (NE).

131 2.4 Description of the automated method

132 Our automatic method selects the start time, peak time and end time of negative NAIS ions in the size range 2 – 4 nm. The
133 growth to an event is confirmed by an accompanying peak in the 7 - 25 nm particles measured by the NAIS. The outcome of
134 the automatic method is the classification of days into the four classes, as well as a time series that identifies the time period
135 of regional events and ion bursts in Hyttiälä (Pathways RE and IB in Figure 1).

136 First, to investigate the appearance of 2 – 4 nm ions, the precipitation time stamps are excluded from our analysis as they
137 interfere with the ion data (Leino et al., 2016), resulting in misinterpretations. After that, the ion concentrations are smoothed
138 using Savitsky-Golay filter (DeSerio, 2008). We then search for an increase in the ion concentration that lasts for 12
139 consecutive points (5 minutes each) above a threshold value and reaches values greater than 20 cm⁻³ (Leino et al., 2016). A
140 maximum of 3 drops below the threshold value are allowed (Figure 2A). Finally, the method looks for a peak in the 7 - 25 nm
141 particle concentration to identify the appearance of a growth phase (Figure 2B). The peak requires 15 consecutive points (5
142 minutes each) having concentrations larger than the threshold value and reaching a value larger than 3000 cm⁻³. Also, a
143 maximum of 3 drops below the threshold value are allowed. Accordingly, each time stamp is classified.

144 2.5 Start time, peak time and end time determination

145 The start time, peak times and end times for regional events and ion bursts are defined based on the 2 – 4 nm ion concentration
146 as follows: i) The start time is the first crossing of the threshold line which lasts for more than 12 consecutive points, ii) the
147 peak time is when the concentration reaches the maximum and iii) the end time is the first trough after crossing the threshold
148 line into lower concentrations which remains below the threshold for more than 3 consecutive points. An example day is
149 demonstrated in Figure 2A. The threshold is taken as the 2 – 4 nm ion concentration averaged over the time period 00:00–
150 04:00 multiplied by a scaling factor of 7. Our scaling factor was determined after we did a comparison with the manual
151 classification of the data for the years 2013–2014.

152 3 Results and Discussion

153 3.1 Event Classification

154 Our classification categorizes the days in Hyttiälä into four different categories following the pathway chart in Figure 1. Type
155 RE, or regional NPF events, are those which are initiated over a large area including the measurement location and the particles
156 continue to grow to bigger sizes. The type TE, or transported events (also known as tail events by Buenrostro Mazon et al.
157 (2009)), are events whose beginning is not detected as it does not occur at the immediate vicinity of our measurement site.



158 Such events could be attributed to events that were initiated outside our measurement site and transported to Hyytiälä (Leino
159 et al. 2018). The aforementioned hypotheses could explain the observation that TE typically occur at around midday or later
160 in the afternoon, while RE tend to occur concurrent with sunrise. The type IB, or ion bursts, are attempts of NPF, during
161 which clusters form in Hyytiälä, however, they do not grow beyond a few nanometers in diameter. Changes in atmospheric
162 conditions that could cause the limited, or interrupted, growth of the clusters are assessed in more detail in section 3.3. Finally,
163 non-events (NE) are days for which we do not observe a forming mode of 2 – 4 nm ions nor a growing mode of 7 - 25 particles.

164 3.2 Frequency of Events

165 For 10 years of data (2006 – 2016), excluding the days with missing NAIS data when the instrument was under maintenance
166 or on campaigns, we classified a total of 2134 days. Using our refined classification method, we were able to classify the days
167 into 4 categories as follows (Figure 3): 551 RE (24%), 410 TE (18%), 415 IB (18%) and 938 NE (40%). This refined
168 classification is able to classify all days into categories and thus eliminate the undefined days that usually constitute around
169 40% of all the days in our location (Dal Maso et al., 2005; Buenrostro Mazon et al., 2009).

170 Moreover, we studied the inter-annual variation of each of the classes (Figure 4A). In general, RE constitute 20-30% of the
171 total classified days. In 2006, the measurement started in September, which explains a lower fraction of RE. The gap in the
172 analysis in 2008 is explained by a campaign during which the NAIS data is not available (Manninen et al., 2010). The data in
173 2009 includes data from spring only, which explains the high frequency of RE in 2009. While we can observe changes in the
174 frequency of RE between the years, no clear trend exists. The annual variation of TE follows that of RE, also with no specific
175 trend over the years. The type IB appears to have an almost constant fraction over the years. Finally, NE constitute between
176 40 and 50% of the days, except in 2009 which has the bias for spring favoring RE.

177 The monthly variation of RE follows the typical yearly cycle of NPF, with a peak in spring, followed by a smaller peak in
178 autumn (Dal Maso et al., 2005; Nieminen et al., 2014; Dada et al., 2017). Interestingly, the refined classification shows that the
179 events occurring in spring are mostly RE while those in autumn are dominated by TE. Additionally, RE rarely occur in winter,
180 appearing on less than 5% of the days. IB have a steady 10-20% occurrence during the year. Finally, NE occur on 60 to 70%
181 of winter days and less than 30% during spring. Interestingly, while previously it was understood that summer is dominated
182 by NE (Nieminen et al., 2014; Dada et al., 2017), the refined classification shows that both TE and IB are frequent during
183 summer, complementing observations by Buenrostro Mazon et al. (2011) who reported ‘failed events’ during summer.

184

185 3.3 Characteristics of RE, TE, IB and NE

186 For a regional event to take place, favorable conditions need to be present. These include a low condensation sink, low relative
187 humidity, moderate temperature and plenty of radiation available during a clear sky (Dada et al., 2017; Hyvönen et al.,
188 2005; Nieminen et al., 2014; Nieminen et al., 2015). In Figure 5, we present the characteristics of each type of event classified
189 in terms of Condensation Sink (CS), relative humidity (RH), Temperature (T) and Cloudiness (P). The data in the plots
190 represent half-hour averages of each variable between 7:00 and 12:00 during spring (March – May). We chose this season in
191 order to capture the maximum NPF events and this time window in order to be consistent between all four studied classes. As
192 expected, the median CS observed on RE was $1.7 \times 10^{-3} \text{ s}^{-1}$ which is a factor of 2 lower than CS observed on TE days or on
193 NE days ($3 \times 10^{-3} \text{ s}^{-1}$). To our understanding, high CS inhibits NPF, so that its higher values during the days classified as TE
194 forbid the initial formation of particles at the measurement site. IB, on the other hand, are potential regional events whose
195 growth has been interrupted. Since the median CS during IB was not high ($2.5 \times 10^{-3} \text{ s}^{-1}$), it does not explain the discontinuous
196 growth of the clusters during these events. We proceed to study the effect of T on the occurrence of each class of events. Since
197 the data in Figure 5 are measurements during spring, the median value of temperature (2-7 °C) was rather similar on all days
198 and no specific trend or exception could be found.

199 In addition to CS and T , RH and cloudiness (P) play an important role in the occurrence of NPF (Dada et al., 2017; Hamed et
200 al., 2011). A regional NPF event is more likely to occur on a clear-sky day rather than on a cloudy day. This conclusion is
201 demonstrated nicely in Figure 5 which shows that the median value of P was close to 0.8 on the RE days and closer to 0.3 on
202 NE day. TE usually took place when the conditions within the boundary layer were not favorable for a regional NPF to occur.
203 However, the particle growth was much less sensitive to environmental conditions: a particle growth was often observed
204 during all times of day and in every season, also on days (and nights) when NPF did not take place (Paasonen et al., 2018).



205 Combined with a higher CS, the value of P was much lower on TE days than on RE days, describing a semi-cloudy day
206 unfavorable for NPF to occur within the boundary layer, which could result in the occurrence of a TE in locations where the
207 conditions are conducive enough to NPF. It is, however, important to mention that it is possible to have a regional NPF episode
208 taking place simultaneously with a transported one, and when the latter is transported it gets mixed with the regional NPF so
209 that this situation will be classified as a RE. Finally, since ion bursts are attempts of an event but do not grow, an interrupted
210 clear sky could explain this phenomenon: for instance a sudden appearance of a cloud would result in the interruption of NPF
211 (Baranizadeh et al., 2014), which then remains as an ion burst only. Finally, the RH, which in general correlates with
212 cloudiness, showed a nice pattern between the event classes: RH was the lowest for RE and the highest for NE, and it fairly
213 reflects cloudiness.

214 3.4 Start times, peak time and end time of RE

215 Our method makes it possible to detect the start, peak and end times of every regional event classified during our study period.
216 Although several previous studies state that the occurrence of NPF starts with sunrise and peaks around midday, very few
217 investigations have considered occurrence times accurately. We derived the start, peak and end times from 2 - 4 nm ions
218 automatically, as mentioned in sections 2.4 and 2.5. Our results (Figure 6) show that indeed RE tended occur after sunrise and
219 prior to noon, with the maximum number of days occurring between sunrise and 5 hours past sunrise. The peak times of the
220 events had the most frequent occurrence at 5 to 6 hours after sunrise, which is between 10:30 and 11:30 local time,
221 complementing our previous assumption that NPF peaks before noon. Finally, the ending times of the events had the most
222 frequent occurrence at 10 hours after sunrise. The importance of the identification of the exact start and end times of the
223 process helps to increase our understanding on the processes governing the NPF phenomenon. More specifically, they allow
224 forming a time series where NPF is separated from non-event times, making it possible to compare the parameters responsible
225 for the NPF process within appropriate time frames.

226 3.5 Comparison to previous classification

227 In order to estimate the goodness of our automatic method, it is crucial to compare our results with the previous classifications
228 (Dal Maso et al., 2005; Kulmala et al., 2012). Although such a comparison is not straightforward, we show one version of
229 such a comparison in Figure 7. On the x-axis, the original classified days are shown, and the refined classes are shown on the
230 y-axis as a fraction of each original class. For example, 65% of the originally-classified event days (event days make 25% of
231 the total days in Hyytiälä according to the original classification) were found to be RE, 10% were TE and 14% were IB. The
232 remaining 11% were considered as misclassified or bad data (by manual classification) and were excluded from the plot. In
233 total, our automatic method was able to classify 89% of the original NPF events into some of the new event classes (RE, TE
234 or IB). The original non-events (which made 40% of the total days) were split between the TE (20%), IB (19%) and NE
235 (53%). The remaining 8% were bad data according to the manual classification and were excluded from the plot.

236 Finally, undefined days, which according to the traditional classification were 35% of the total days, were split between all
237 the classes. Our results show that 17% of those were RE, 21% were TE, 19% were IB and 42% were non-events. Those days
238 were usually excluded from further analysis because they did not belong to a defined class according to the original
239 classification method. Previous extensive studies of undefined days in Hyytiälä by Buenrostro Mazon et al. (2009) showed
240 that a fraction of undefined days resembles interrupted events which, in our case, were 83% of the days (TE, IB or NE), and
241 which all in all were related to unfavorable conditions for regional NPF. The interruption mechanisms may include appearance
242 of clouds (Dada et al., 2017), resulting in decreased radiation essential for particle formation and growth (Jokinen et al., 2017).
243 Others include a change of arriving air masses from a clean to a rather polluted sector (Sogacheva et al., 2005). Also, the
244 growth can be interrupted by a sudden appearance of a cloud (Baranizadeh et al., 2014; Dada et al., 2017).

245 4 Conclusions

246 Using 10 years of measurement using the NAIS at SMEAR II station, we were able to create an automated method to classify
247 days into 4 classes based on their ion (2 - 4 nm) and particle (7 - 25 nm) number concentrations, including regional events,
248 transported events, ion bursts and non-events. Our method minimizes the efforts used in manual day-by-day classification as
249 well as the errors due to human bias. In addition, our method allows for the complete classification (sub-3 nm) of all days, i.e.
250 reduces the number of previously known 'undefined days', which have always been excluded from previous analyses.



251 Our results show that on ~ 40% of the days during spring in Hyytiälä, a regional NPF event occurs and is characterized by a
252 set of favorable conditions, such as a clear sky, low condensation sink, medium temperature and low relative humidity. On
253 the contrary, NE were ~25 % of the days and were characterized by a complete cloud cover, high RH and high CS.
254 Interestingly, TE and IB fall in the category between RE and NE in this respect. While IB are interrupted growth of initially
255 started RE due to a probable change to polluted air mass or an appearance of a cloud, TE occurred on days when there was
256 little chance for the cluster to form within our measurement location but still they had a chance to grow if reaching our site.
257 Both IB and TE were characterized by intermediate values of CS, RH and P compared with RE and NE. Moreover, using the
258 new method we are able to identify the start time, peak time and end time of events occurring in Hyytiälä. Our results show
259 that most RE started within 5 hours from the sunrise, peaked before noon, and ended 10 hours after sunrise. Finally, with
260 small changes the classification method can be applied to other places around the globe where NPF takes place providing
261 deeper understanding yet less effort for atmospheric scientists.

262



263

264 *Acknowledgements:* Lubna Dada acknowledges the doctoral programme in Atmospheric Sciences (ATM-DP, University of
265 Helsinki) for financial support. This project has received funding from the European Union's Horizon 2020 research. This
266 work was supported by the European Commission via projects ACTRIS2, European Research Council via ATM-GTP
267 (742206), and Academy of Finland Centre of Excellence in Atmospheric Sciences (grant number: 272041).

268 *Data availability:* Data measured at the SMEAR II station are available on the webpage: <http://avaa.tdata.fi/web/smart/>. The
269 classification, start times, peak times and end times are available from Lubna Dada (lubna.dada@helsinki.fi) upon request.

270

271 References

272 Aalto, P., Hämeri, K., Becker, E., Weber, R., Salm, J., Mäkelä, J. M., Hoell, C., O'dowd, C. D., Hansson, H.-C., Väkevä, M.,
273 Koponen, I. K., Buzorius, G., and Kulmala, M.: Physical characterization of aerosol particles during nucleation
274 events, *Tellus B*, 53, 344-358 [10.1034/j.1600-0889.2001.530403.x](https://doi.org/10.1034/j.1600-0889.2001.530403.x), 2001.

275 Artaxo, P., Rizzo, L. V., Brito, J. F., Barbosa, H. M., Arana, A., Sena, E. T., Cirino, G. G., Bastos, W., Martin, S. T., and
276 Andreae, M. O.: Atmospheric aerosols in Amazonia and land use change: from natural biogenic to biomass burning
277 conditions, *Faraday discussions*, 165, 203-235, 2013.

278 Asmi, A., Wiedensohler, A., Laj, P., Fjaeraa, A.-M., Sellegri, K., Birmili, W., Weingartner, E., Baltensperger, U., Zdimal, V.,
279 and Zikova, N.: Number size distributions and seasonality of submicron particles in Europe 2008–2009, *Atmos.*
280 *Chem. Phys.*, 11, 5505-5538, [10.5194/acp-11-5505-2011](https://doi.org/10.5194/acp-11-5505-2011), 2011.

281 Asmi, E., Kondratyev, V., Brus, D., Laurila, T., Lihavainen, H., Backman, J., Vakkari, V., Aurela, M., Hatakka, J., Viisanen,
282 Y., Uttal, T., Ivakhov, V., and Makshtas, A.: Aerosol size distribution seasonal characteristics measured in Tiksi,
283 Russian Arctic, *Atmos. Chem. Phys.*, 16, 1271-1287, [10.5194/acp-16-1271-2016](https://doi.org/10.5194/acp-16-1271-2016), 2016.

284 Baranizadeh, E., Arola, A., Hamed, A., Nieminen, T., Mikkonen, S., Virtanen, A., Kulmala, M., Lehtinen, K., and Laaksonen,
285 A.: The effect of cloudiness on new-particle formation: investigation of radiation levels, *Boreal Env. Res.*, 19, 343-
286 354, 2014.

287 Bianchi, F., Tröstl, J., Junninen, H., Frege, C., Henne, S., Hoyle, C., Molteni, U., Herrmann, E., Adamov, A., Bukowiecki,
288 N., Chen, X., Duplissy, J., Gysel, M., Hutterli, M., Kangasluoma, J., Kontkanen, J., Kürten, A., Manninen, H. E.,
289 Münch, S., Peräkylä, O., Petäjä, T., Rondo, L., Williamson, C., Weingartner, E., Curtius, J., Worsnop, D. R.,
290 Kulmala, M., Dommen, J., and Baltensperger, U.: New particle formation in the free troposphere: A question of
291 chemistry and timing, *Science*, 352, 1109-1112, [10.1126/science.aad5456](https://doi.org/10.1126/science.aad5456), 2016.

292 Buenrostro Mazon, S., Riipinen, I., Schultz, D., Valtanen, M., Maso, M. D., Sogacheva, L., Junninen, H., Nieminen, T.,
293 Kerminen, V.-M., and Kulmala, M.: Classifying previously undefined days from eleven years of aerosol-particle-
294 size distribution data from the SMEAR II station, Hyytiälä, Finland, *Atmos. Chem. Phys.*, 9, 667-676, [10.5194/acp-9-667-2009](https://doi.org/10.5194/acp-9-667-2009), 2009.

296 Dada, L., Paasonen, P., Nieminen, T., Buenrostro Mazon, S., Kontkanen, J., Peräkylä, O., Lehtipalo, K., Hussein, T., Petäjä,
297 T., Kerminen, V. M., Bäck, J., and Kulmala, M.: Long-term analysis of clear-sky new particle formation events and
298 nonevents in Hyytiälä, *Atmos. Chem. Phys.*, 17, 6227-6241, [10.5194/acp-17-6227-2017](https://doi.org/10.5194/acp-17-6227-2017), 2017.

299 Dal Maso, M., Kulmala, M., Riipinen, I., Wagner, R., Hussein, T., Aalto, P. P., and Lehtinen, K. E.: Formation and growth
300 of fresh atmospheric aerosols: eight years of aerosol size distribution data from SMEAR II, Hyytiälä, Finland, *Boreal*
301 *Env. Res.*, 10, 323, 2005.

302 DeSerio, R.: Savitsky-Golay Filters, 2008.



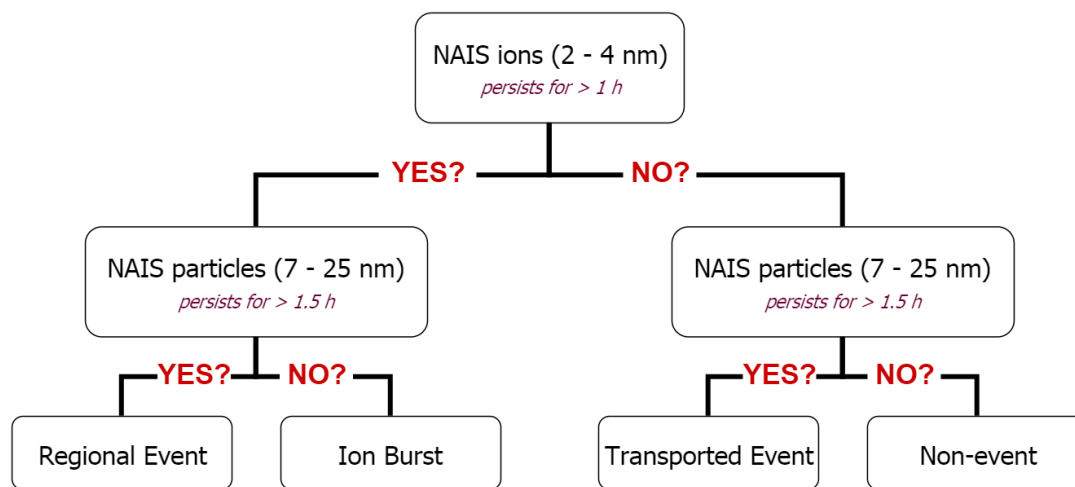
- 303 Hamed, A., Korhonen, H., Sihto, S. L., Joutsensaari, J., Järvinen, H., Petäjä, T., Arnold, F., Nieminen, T., Kulmala, M., and
304 Smith, J. N.: The role of relative humidity in continental new particle formation, *Journal of Geophysical Research:*
305 *Atmospheres*, 116, 2011.
- 306 Hari, P., and Kulmala, M.: Station for measuring ecosystem-atmosphere relations, *Boreal Env. Res.*, 10, 315-322, 2005.
- 307 Hyvönen, S., Junninen, H., Laakso, L., Maso, M. D., Grönholm, T., Bonn, B., Keronen, P., Aalto, P., Hiltunen, V., Pohja, T.,
308 Launiainen, S., Hari, P., Mannila, H., and Kulmala, M.: A look at aerosol formation using data mining techniques,
309 *Atmos. Chem. Phys.*, 5, 3345-3356, 10.5194/acp-5-3345-2005, 2005.
- 310 Jokinen, T., Kontkanen, J., Lehtipalo, K., Manninen, H. E., Aalto, J., Porcar-Castell, A., Garmash, O., Nieminen, T., Ehn, M.,
311 and Kangasluoma, J.: Solar eclipse demonstrating the importance of photochemistry in new particle formation,
312 *Scientific Reports*, 7, 45707, 2017.
- 313 Kerminen V.-M., C., X., Vakkari, V., Petäjä, T., Kulmala, M. and Bianchi, F.: Atmospheric new particle formation: review of
314 observations, *Environmental Research Letters* (Submitted), 2018.
- 315 Kulmala, M., Alekseychik, P., Paramonov, M., Laurila, T., Asmi, E., Arneth, A., Zilitinkevich, S., and Kerminen, V.-M.: On
316 measurements of aerosol particles and greenhouse gases in Siberia and future research needs, *Boreal Environment*
317 *Research*, 16, 2011.
- 318 Kulmala, M., Petäjä, T., Nieminen, T., Sipilä, M., Manninen, H. E., Lehtipalo, K., Dal Maso, M., Aalto, P. P., Junninen, H.,
319 and Paasonen, P.: Measurement of the nucleation of atmospheric aerosol particles, *Nature protocols*, 7, 1651-1667,
320 10.1038/nprot.2012.091, 2012.
- 321 Kulmala, M., Kontkanen, J., Junninen, H., Lehtipalo, K., Manninen, H. E., Nieminen, T., Petäjä, T., Sipilä, M., Schobesberger,
322 S., Rantala, P., Franchin, A., Jokinen, T., Järvinen, E., Äijälä, M., Kangasluoma, J., Hakala, J., Aalto, P., Paasonen,
323 P., Mikkilä, J., Vanhanen, J., Aalto, J., Hakola, H., Makkonen, U., Ruuskanen, T., Mauldin, R. r., Duplissy, J.,
324 Vehkamäki, H., Bäck, J., Kortelainen, A., Riipinen, I., Kurtén, T., Johnston, M., Smith, J., Ehn, M., Mentel, T.,
325 Lehtinen, K., Laaksonen, A., Kerminen, V., and Worsnop, D.: Direct observations of atmospheric aerosol nucleation,
326 *Science*, 339, 943-946, 10.1126/science.1227385, 2013.
- 327 Kulmala, M., Petäjä, T., Kerminen, V.-M., Kujansuu, J., Ruuskanen, T., Ding, A., Nie, W., Hu, M., Wang, Z., Wu, Z., Wang,
328 L., and Worsnop, D. R.: On secondary new particle formation in China, *Frontiers of Environmental Science &*
329 *Engineering*, 10, 8, 10.1007/s11783-016-0850-1, 2016.
- 330 Kulmala, M., Kerminen, V.-M., Petäjä, T., Ding, A., and Wang, L.: Atmospheric gas-to-particle conversion: why NPF events
331 are observed in megacities?, *Faraday discussions*, 200, 271-288, 2017.
- 332 Kulmala, M.: Build a global Earth observatory, *Nature*, 553, 21-23, 2018.
- 333 Leino, K., Nieminen, T., Manninen, H. E., Petäjä, T., Kerminen, V.-M., and Kulmala, M.: Intermediate ions as a strong
334 indicator of new particle formation bursts in a boreal forest, 2016.
- 335 Leino, K., Lampilahti, J., Poutanen, P., Väänänen, R., Manninen, A., Mazon, S. B., Dada, L., Nikandrova, A., Wimmer, D.,
336 Aalto, P. P., Ahonen, L. R., Enroth, J., Kangasluoma, J., Keronen, P., Korhonen, F., Laakso, H., Matilainen, T.,
337 Siivola, E., Manninen, H. E., Lehtipalo, K., Kerminen, V.-M., Petäjä, T., and Kulmala, M.: Vertical profiles of sub-
338 3 nm particles over the boreal forest *Atmos. Chem. Phys. Discuss.* (Submitted), 2018.
- 339 Manninen, H. E., Petäjä, T., Asmi, E., Riipinen, I., Nieminen, T., Mikkilä, J., Hörrak, U., Mirme, A., Mirme, S., and Laakso,
340 L.: Long-term field measurements of charged and neutral clusters using Neutral cluster and Air Ion Spectrometer
341 (NAIS), *Boreal Environ. Res.*, 14, 591-605, 2009.
- 342 Manninen, H. E., Nieminen, T., Asmi, E., Gagné, S., Häkkinen, S., Lehtipalo, K., Aalto, P., Vana, M., Mirme, A., Mirme, S.,
343 Hörrak, U., Plass-Dülmer, C., Stange, G., Kiss, G., Hoffer, A., Törö, N., Moerman, M., Henzing, B., de Leeuw, G.,



- 344 Brinkenberg, M., Kouvarakis, G. N., Bougiatioti, A., Mihalopoulos, N., O'Dowd, C., Ceburnis, D., Arneth, A.,
345 Svenningsson, B., Swietlicki, E., Tarozzi, L., Decesari, S., Facchini, M. C., Birmili, W., Sonntag, A., Wiedensohler,
346 A., Boulon, J., Sellegri, K., Laj, P., Gysel, M., Bukowiecki, N., Weingartner, E., Wehrle, G., Laaksonen, A., Hamed,
347 A., Joutsensaari, J., Petäjä, T., Kerminen, V. M., and Kulmala, M.: EUCAARI ion spectrometer measurements at 12
348 European sites – analysis of new particle formation events, *Atmos. Chem. Phys.*, 10, 7907-7927, 10.5194/acp-10-
349 7907-2010, 2010.
- 350 Manninen, H. E., Mirme, S., Mirme, A., Petäjä, T., and Kulmala, M.: How to reliably detect molecular clusters and nucleation
351 mode particles with Neutral cluster and Air Ion Spectrometer (NAIS), *Atmospheric Measurement Techniques*, 2016.
- 352 Mirme, S., and Mirme, A.: The mathematical principles and design of the NAIS—a spectrometer for the measurement of cluster
353 ion and nanometer aerosol size distributions, *Atmospheric Measurement Techniques*, 6, 1061-1071, 2013.
- 354 Nieminen, T., Asmi, A., Dal Maso, M., Aalto, P. P., Keronen, P., Petäjä, T., Kulmala, M., and Kerminen, V.-M.: Trends in
355 atmospheric new-particle formation: 16 years of observations in a boreal-forest environment, *Boreal Env. Res.*, 19,
356 2014.
- 357 Nieminen, T., Yli-Juuti, T., Manninen, H., Petäjä, T., Kerminen, V.-M., and Kulmala, M.: Technical note: New particle
358 formation event forecasts during PEGASOS–Zeppelin Northern mission 2013 in Hyttiälä, Finland, *Atmos. Chem.*
359 *Phys.*, 15, 12385-12396, 10.5194/acp-15-12385-2015, 2015.
- 360 Paasonen, P., Peltola, M., Kontkanen, J., Junninen, H., Kerminen, V.-M., and Kulmala, M.: Comprehensive analysis of
361 particle growth rates from nucleation mode to cloud condensation nuclei in Boreal forest, *Atmos. Chem. Phys.*
362 *Discuss.* (Submitted), 2018.
- 363 Sogacheva, L., Dal Maso, M., Kerminen, V.-M., and Kulmala, M.: Probability of nucleation events and aerosol particle
364 concentration in different air mass types arriving at Hyttiälä, southern Finland, based on back trajectories analysis,
365 *Boreal Env. Res.*, 10, 2005.
- 366 Spracklen, D. V., Carslaw, K. S., Merikanto, J., Mann, G. W., Reddington, C. L., Pickering, S., Ogren, J. A., Andrews, E.,
367 Baltensperger, U., Weingartner, E., Boy, M., Kulmala, M., Laakso, L., Lihavainen, H., Kivekäs, N., Komppula, M.,
368 Mihalopoulos, N., Kouvarakis, G., Jennings, S. G., O'Dowd, C., Birmili, W., Wiedensohler, A., Weller, R., Gras, J.,
369 Laj, P., Sellegri, K., Bonn, B., Krejci, R., Laaksonen, A., Hamed, A., Minikin, A., Harrison, R. M., Talbot, R., and
370 Sun, J.: Explaining global surface aerosol number concentrations in terms of primary emissions and particle
371 formation, *Atmos. Chem. Phys.*, 10, 4775-4793, 10.5194/acp-10-4775-2010, 2010.
- 372 Wang, Z., Wu, Z., Yue, D., Shang, D., Guo, S., Sun, J., Ding, A., Wang, L., Jiang, J., and Guo, H.: New particle formation in
373 China: Current knowledge and further directions, *Science of the Total Environment*, 577, 258-266, 2017.
- 374 Wimmer, D., Buenrostro Mazon, S., Manninen, H. E., Kangasluoma, J., Franchin, A., Nieminen, T., Backmann, J., Wang, J.,
375 Kuang, C., Krejci, R., Brito, J., Goncalves Morais, F., Martin, S. T., Artaxo, P., Kulmala, M., Kerminen, V. M., and
376 Petäjä, T.: Direct observation of molecular clusters and nucleation mode particles in the Amazon, *Atmos. Chem.*
377 *Phys. Discuss.*, 2017, 1-37, 10.5194/acp-2017-782, 2017.



378



379

380 *Figure 1 A flow chart for the decision path during event classification in Hyytiälä using new classification method.*

381



382

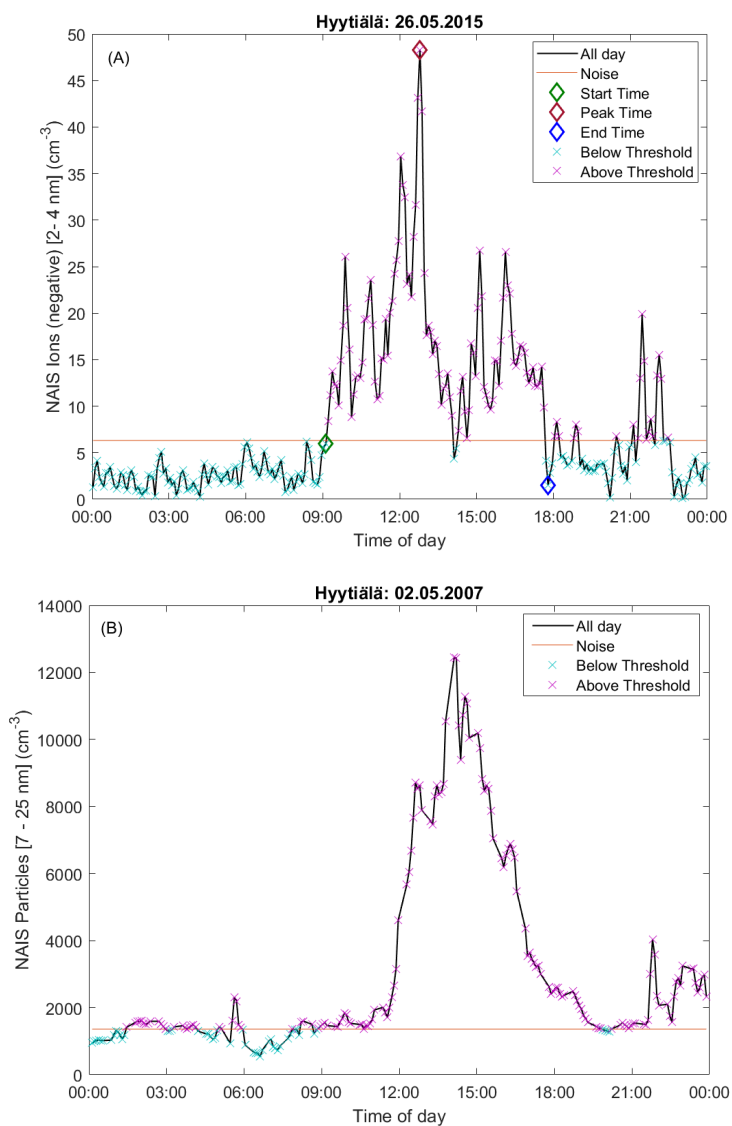
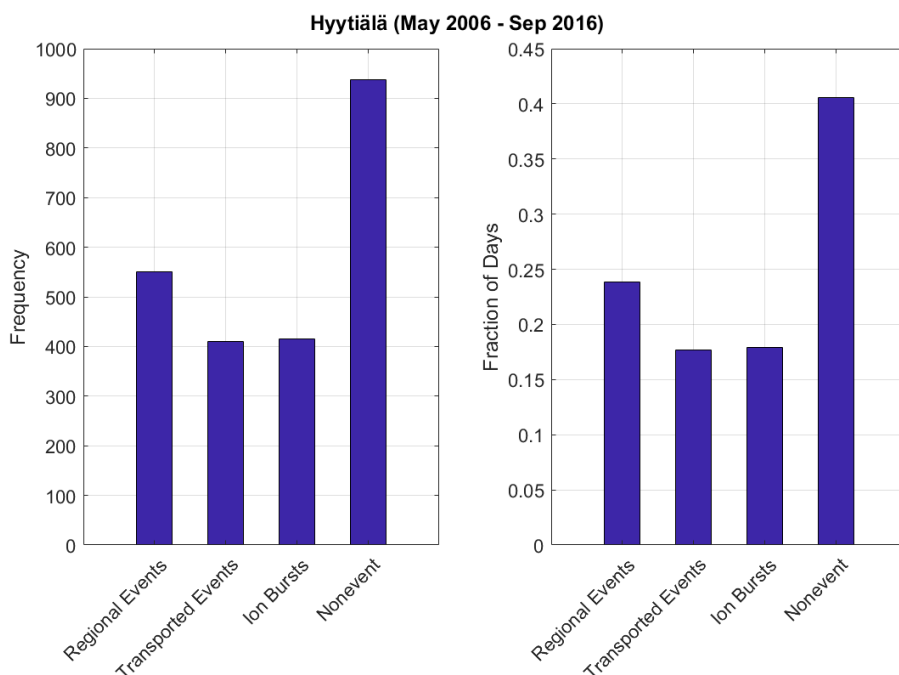


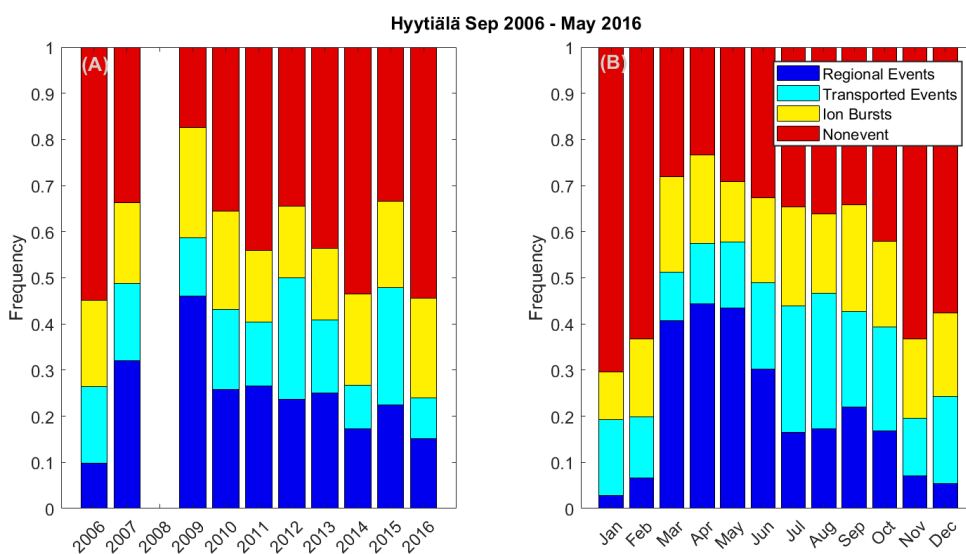
Figure 2 Automatic method applied to (A) 2 – 4 nm ions (negative) example, ion concentration passed threshold and persisted > 1 hour and (B) 7 – 25 nm particles example, particle concentration passed threshold and persisted for > 1.5 hours.

383



384

385 **Figure 3** Frequency and fraction of events, ions burst and non-events in Hyttiälä using the new classification method.



386

387 **Figure 4** (A) Yearly and (B) monthly fraction of days classified as Regional events (RE), Transported events (TE), Ion
 388 bursts (IB), and non-events (NE) using the new classification method. The data of year 2009 is bias to spring months,
 389 which could explain the much higher number of events. No data was available during 2008.

390

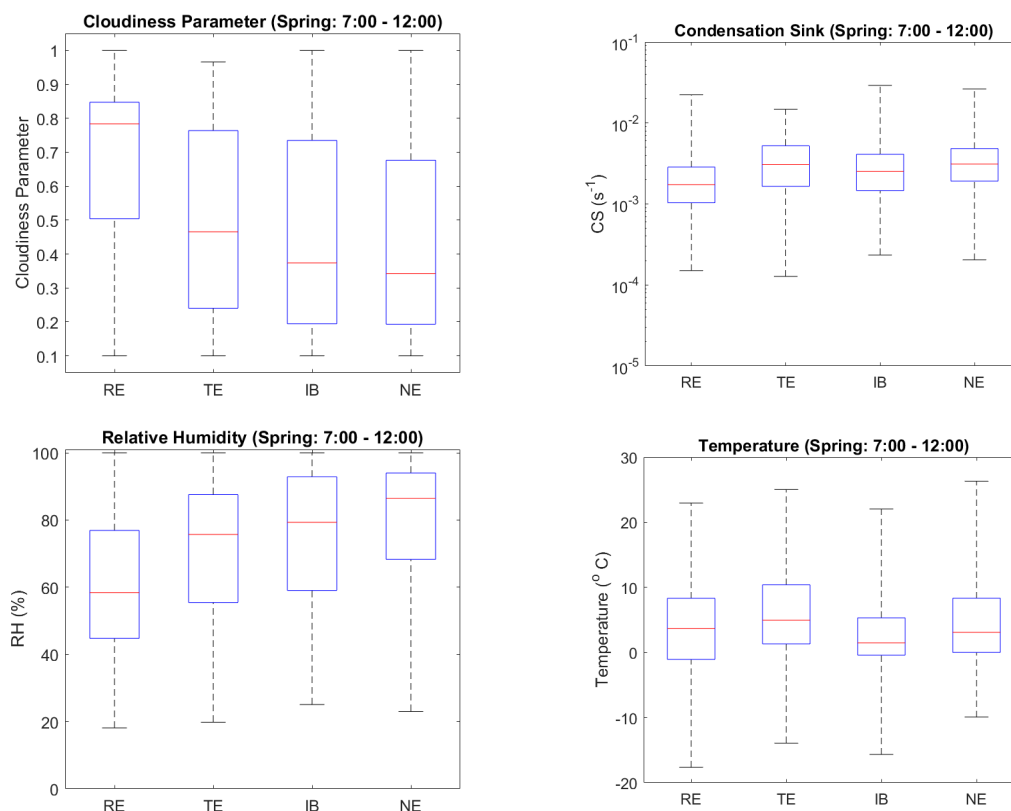


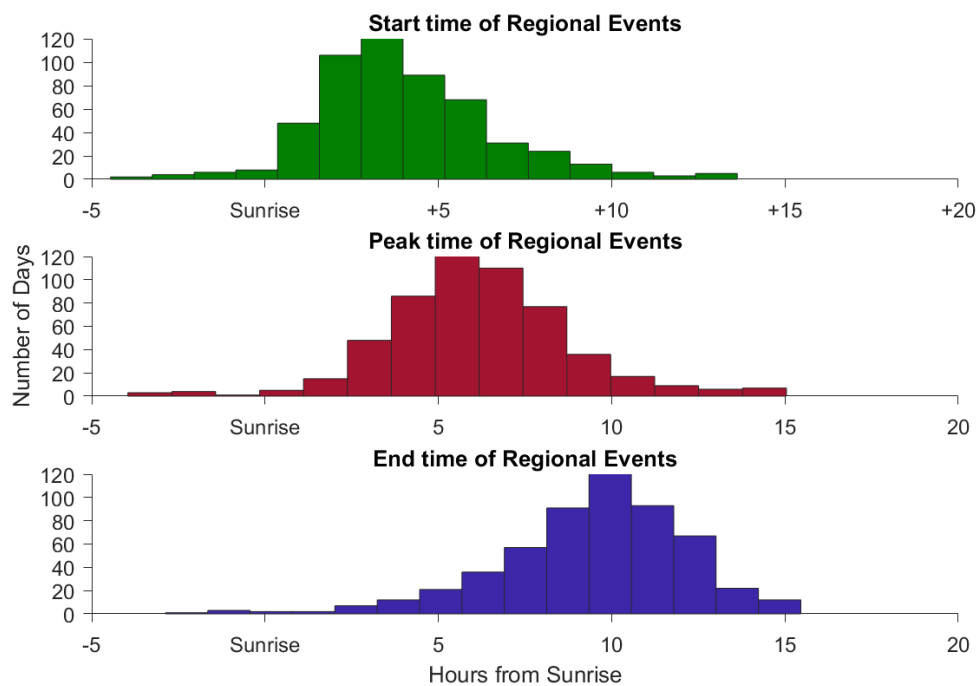
Figure 5 (A) Cloudiness parameter, (B) condensation sink, (C) Relative humidity and (D) Temperature during different days classified with the new classification method for Spring (Mar-May) of 2006-2016 during maximum NPF window (7:00 – 12:00). The acronyms RE, TE, IB and NE stand for regional events, transported events, ions bursts and non-events, respectively. The red line represents the median of the data and the lower and upper edges of the box represent 25th and 75th percentiles of the data respectively. The lines extending from the central box represent the minimum and the maximum of the data inclusive.

391

392

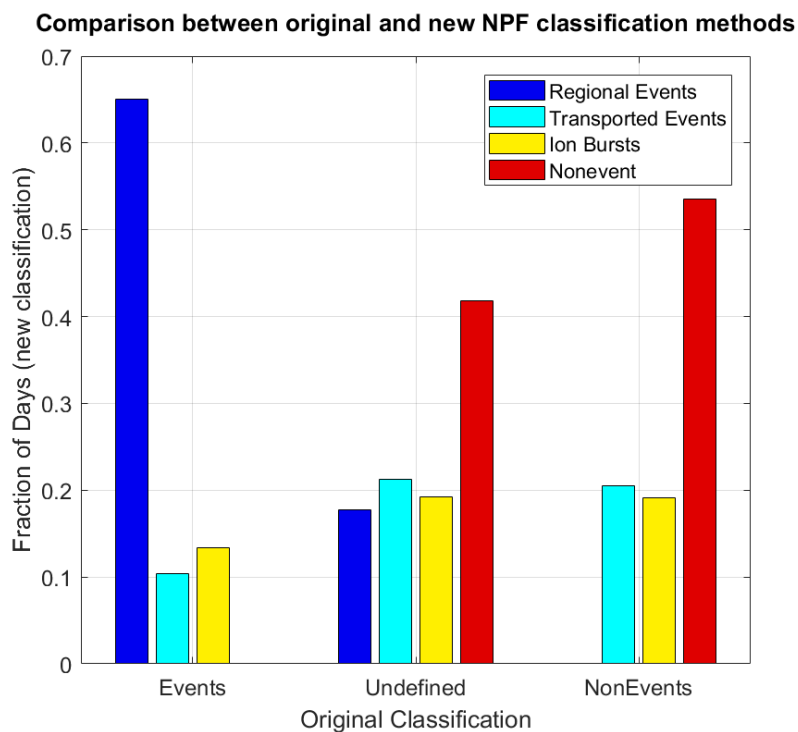


393



394

395 *Figure 6 Frequency of days at which regional events start, peak and end past sunrise. For example, most events start*
396 *within 5 hours from sunrise.*



397

398 *Figure 7 Comparison between original and new NPF classification methods. The refined classification matches 94% with*
 399 *original event and non-event classification.*

400

401